

RSC Advances



This is an *Accepted Manuscript*, which has been through the Royal Society of Chemistry peer review process and has been accepted for publication.

Accepted Manuscripts are published online shortly after acceptance, before technical editing, formatting and proof reading. Using this free service, authors can make their results available to the community, in citable form, before we publish the edited article. This *Accepted Manuscript* will be replaced by the edited, formatted and paginated article as soon as this is available.

You can find more information about *Accepted Manuscripts* in the [Information for Authors](#).

Please note that technical editing may introduce minor changes to the text and/or graphics, which may alter content. The journal's standard [Terms & Conditions](#) and the [Ethical guidelines](#) still apply. In no event shall the Royal Society of Chemistry be held responsible for any errors or omissions in this *Accepted Manuscript* or any consequences arising from the use of any information it contains.



Biohybrid hematopoietic niche for expansion of hematopoietic stem/progenitor cells by using geometrically controlled fibrous layers

Received 00th January 20xx,
Accepted 00th January 20xx

DOI: 10.1039/x0xx00000x

www.rsc.org/

Onon Batnyam^a, Harue Shimizu^a, Koichi Saito^b, Tomohiko Ishida^c, Shin-ichiro Suye^a, Satoshi Fujita^{*a}

The expansion of hematopoietic stem/progenitor cells (HSPCs), which can give rise of all types of mature blood cells, is one of the actual challenges of regenerative medicine. In this study, we propose a construction of 3D hematopoietic niche for the coculture of HSPCs and mesenchymal stem cells, which was prepared from geometrically controlled electrospun fibrous layers. The proliferation activity, retention of CD34⁺CD38⁻ immunophenotype and multipotency of the HSPCs in artificial hematopoietic niche were analyzed by FACS and colony-forming unit assay. Results showed that the 3D biohybrid hematopoietic niche has a capacity to support self-renewal of HSPCs, maintaining their primitive phenotype and accommodate a large number of expanded cells. The geometry of the artificial niche served as a physical cue that controlled chemical signals to facilitate successful *in vitro* expansion and retention of HSPCs potential to differentiate into various lineages.

1 Introduction

Nowadays, the hematopoietic stem/progenitor cells (HSPCs) that have the property of self-renewal and differentiation into all types of mature blood cells is becoming one of the essential tools in regenerative medicine.¹ The transplantation of HSPCs has become an important curative standard for hematological conditions such as multiple myeloma, non-Hodgkin's lymphoma, Hodgkin's lymphoma, β -thalassemia and sickle cell anemia.²⁻⁴ HSPCs can be harvested from healthy donor's pelvis, femur, and sternum by bone marrow (BM) aspiration, but this method involves a high risk for the donor.⁵⁻⁷ Next conventional source of HSPCs is peripheral blood (PB), but the cell collection procedure from this source is not easy and has a risk for a donor as well.⁸ PB stem cells also have a high chance to cause graft-versus-host diseases, which is associated with lymphocyte subpopulation, particularly T-lymphocytes.⁹ On the other hand, harvesting HSPCs from the umbilical cord blood (CB) has several advantages as source is readily available, involves a non-invasive collection procedure, and obtained cells are better tolerated across the human leukocyte antigens barrier. Moreover, the proliferative capacity of CB derived HSPCs (CB-HSPCs) is superior to that of cells from BM.¹⁰ Unfortunately, HSPCs yield from a single donor CB is low, thus *in vitro* expansion of HSPCs is required to improve the clinical outcome of allogeneic HSPCs

transplantation.

Previous studies have reported that *in vitro* 100-fold expansion of CD34⁺ cells was obtained by culturing human CD34⁺CD38⁻ HSPCs with immobilized Notch ligand Delta-1,¹¹ and another study reported reprogramming of human endothelial cells with specific transcription factors such as FOSB, growth factor independent 1 (GFI1), RUNX1 and SPI1, combined with the signals from E4ORF1 endothelial cells led to induced HSPCs capable of engrafting to immunodeficient mice.¹² However, these methods are laborious and expensive. Other expansion methods involve utilization of coculture systems, where HSPCs seeded on top of mesenchymal stem cells (MSCs) monolayer.^{13, 14} In this system, the yield of expanded HSPCs is low and requires periodic subculturing as well as these conventional two-dimensional (2D) culture conditions are entirely different from the bone epiphyseal and metaphyseal regions, where homeostatic HSPCs are distributed.^{15, 16} Therefore, the high-yield *in vitro* expansion conditions of HSPCs should closely mimic a natural three-dimensional (3D) microenvironment, called hematopoietic niche, where the combination of soluble factors, intrinsic signaling pathways, adhesion molecules, local oxygen tension and cell-to-cell contact regulates the balance and homeostasis of HSPCs, self-renewal, proliferation and differentiation.^{14, 17-20} Many of those factors are facilitated by MSCs in hematopoietic niche or by their progeny committed to osteoblasts, which play an important role in nurturing of HSPCs in hematopoietic niche not only by supporting their proliferation, but also maintaining their primitive immunophenotype over a higher number of population doublings.^{13, 21} Another important aspect of hematopoietic niche is a 3D extracellular matrix (ECM) that provides mechanical support to all constituent of the niche. In our previous studies, we have unveiled a potential of electrospun fiber

^a Department of Frontier Fiber Technology and Science, Graduate School of Engineering, University of Fukui, Fukui, 910-8507, Japan.

^b Research Center for Regenerative Medicine, ELL, Inc. Tokyo 100-8246, Japan.

^c Department of Obstetrics and Gynaecology, Itabashi Chuo Medical Center, Tokyo 174-0051, Japan.

1 scaffolds geometry in controlling MSCs differentiation through
2 mechanotransduction. In the presence of a mixed medium that
3 facilitated both adipogenesis and osteogenesis, the
4 adipogenesis was markedly inhibited on the fiber scaffolds with
5 anisotropic properties supporting uniform osteogenesis,²² which is
6 essential for self-renewal and proliferation of HSPCs in
7 hematopoietic niche.²¹

8 In this study, we have demonstrated a construction of 3D
9 biohybrid hematopoietic niche-like microenvironment for the
10 expansion of CB-HSPCs by fabricating high porous fiber scaffolds
11 with different geometry and MSCs as feeder cells. The advantage of
12 our niche is its beehive-like structure, where overlaid scaffolds can
13 be easily separated from each other allowing convenient and
14 efficient cell harvesting. The self-renewal, retention of CD34⁺CD38⁻
15 immunophenotype and multipotency of the HSPCs cultured in the
16 artificial hematopoietic niches were evaluated by FACS and colony-
17 forming unit assay. Our coculture system was designed to achieve
18 efficient growth of HSPCs in high density by mimicking the
19 microenvironment of hematopoietic niche in bone marrow
20 endosteum.

21

22 Material and methods

23 Materials

24

25 Thermoplastic polyether-polyurethane-elastomer (PU, Mw 146,000,
26 Elastollan® 1180A10) was purchased from BASF (Ludwigshafen,
27 Germany); tetrahydrofuran (THF), *N,N*-dimethylformamide (DMF),
28 were purchased from Wako (Osaka, Japan). All other chemicals and
29 reagents were of analytical grade and were used without further
30 purification.

31

32 Fabrication of electrospun fiber scaffolds

33 Electrospinning solution was prepared by dissolving PU in 95 v/v%
34 THF and 5 v/v% DMF to obtain a final concentration of PU 12.5
35 wt/v%. PU nanofibers were electrospun onto acrylic frames with
36 thickness of 200 μm (Fig. 1A) using a commercialized
37 electrospinning setup (NANON-01A, MECC Co., Ltd., Fukuoka,
38 Japan) which consisted of a closed chamber, high voltage power
39 supply, a rotating collector (φ10 cm), a syringe pump, 5 mL syringe
40 and a 27 G-needle. The applied voltage was set to 30 kV. The
41 distance between the needle tip and collector was kept constant at
42 15 cm. The infusion rate of electrospinning solutions was controlled
43 at 0.2 mL h⁻¹, the collector rotation velocity for transversely
44 isotropic (Scaffold-I) and anisotropic fibers (Scaffold-II) were set at
45 1.5 m s⁻¹ and 0.05 m s⁻¹, respectively. To improve surface
46 hydrophilicity of the fibers and sterilization, oxygen plasma
47 treatment (40 kHz/100 W, 30 s, 0.1 MPa) was carried out by using a
48 plasma reactor (Diener Electronics, Plasma Cleaner Femto,
49 Ebhausen, Germany, chamber size, diameter 95 mm × depth 270
50 mm).

51 Scanning electron microscopy

52 The morphological observations of obtained scaffolds were carried
53 out using scanning electron microscope (SEM, Hitachi S-2600HS,
54 Tokyo, Japan) at an accelerating voltage of 15 kV. Samples were
55 sputtered with Pt/Pd using ion sputter (E-1030, Hitachi, Tokyo,
56 Japan) for 120 s prior to observation. Images of ten randomly
57 selected areas per sample were captured and used for fiber
58 diameter and fiber orientation measurements using Fiji software
59 (Fiji.sc; ImageJ 1.49m, NIH, USA). Fiber orientation was quantified
60 using the second-order parameter, *S*, as follows:

$$61 \quad S = (3\langle \cos^2\vartheta \rangle - 1)/2$$

62 where ϑ is an angle of each fiber and $\langle \cos^2\vartheta \rangle$ is the average of
63 $\cos^2\vartheta$.^{23, 24}

64 Isolation of hematopoietic stem cells from umbilical cord blood

65 Studies were approved by the institutional review board. CB was
66 obtained from healthy donors with their informed consent. The
67 CD34⁺ cell fraction that is rich in HSPCs was isolated from fresh CB
68 as follows; mononuclear cells were isolated by density gradient
69 centrifugation using Lymphoprep (AXIS-SHIELD PoC AS, Oslo,
70 Norway). After washing twice with Dulbecco's phosphate-buffered
71 saline (PBS; Nissui Pharmaceutical Co. Ltd., Tokyo, Japan), CD34⁺
72 cells were isolated by magnetic beads (Direct CD34 Progenitor Cell
73 Isolation Kit; Miltenyi Biotech GmbH, Bergisch Gladbach, Germany)
74 in accordance with the manufacturer's instructions. Isolated CD34⁺
75 cells were cryopreserved using a bovine serum containing cell
76 freezing media (Cellbanker, Nippon Zenyaku Kogyo Co., Ltd.,
77 Fukushima, Japan), and stored in liquid nitrogen until further use.

78 Culture of human mesenchymal stem cells

79 Human bone marrow mesenchymal stem cells (MSCs, Takara Bio,
80 Shiga, Japan) were cultured in Dulbecco's Modified Essential
81 Medium (DMEM; Invitrogen, CA, USA) supplemented with 10% fetal
82 bovine serum (FBS; Sigma-Aldrich, St. Louis, MO, USA), 100 U mL⁻¹
83 penicillin, and 100 μg mL⁻¹ streptomycin (Wako Pure Chemical
84 Industries Ltd., Osaka, Japan). Cultures were incubated in a
85 humidified atmosphere with 5% CO₂ at 37°C. Cells were passaged
86 upon reaching near confluency, and reseeded to a density of 3 × 10³
87 cells per cm². Cells with passage numbers between 2 to 8 were used
88 for further experiments.

89 Coculture of hematopoietic stem cells with mesenchymal stem 90 cells seeded on the layered fiber scaffolds

91 First, MSCs were seeded at a density of 2 × 10⁴ cells per cm² onto
92 prepared electrospun fiber scaffolds, which were washed twice
93 with PBS and once with 10% FBS/DMEM prior cell seeding, and
94 cultured at 37°C for 1 week. Three replicates were carried out in
95 each culture. Then, three layers of MSCs seeded fiber scaffolds
96 were overlaid on each other in 2.5 × 10³ cells mL⁻¹ HSPCs and 2%
97 methylcellulose (#400; Nacalai Tesque, Inc., Kyoto, Japan)
98 containing PBS. Then cells were cocultured in StemPro-34 SFM
99 (Invitrogen, CA, USA) serum-free medium specifically formulated to
100 support the growth of human hematopoietic progenitor cells
101 supplemented with 2 mM L-alanyl-L-glutamine (GLUTAMAX I;

1 Invitrogen, CA, USA), 50 ng mL⁻¹ Flt-3 ligand, 50 ng mL⁻¹ stem cell
 2 factor, and 50 ng mL⁻¹ thrombopoietin (StemSpan CC110; Stemcell
 3 Technologies Inc., Vancouver, Canada). After 1 week of coculture at
 4 37°C under 5% CO₂ in a humidified atmosphere without changing
 5 the culture medium. The control cells were cocultured on
 6 monolayer of MSCs which were seeded in a ϕ 35 mm culture dish.
 7 HSPCs cultured on Scaffold-I were named 3D culture-I (3D-I) and
 8 HSPCs cultured on Scaffold-II were named 3D-II (3D-II). Prior
 9 examinations cells were dissociated using 0.05% trypsin-EDTA
 10 solution (Wako Pure Chemical Industries Ltd., Osaka, Japan) and
 11 characterization by flow cytometry and colony-forming cell assay.

12 Quantitative RT-PCR

13 Gene expression in feeder MSCs was analyzed by quantitative
 14 reverse transcription-polymerase chain reaction (qRT-PCR). Total
 15 RNA was extracted from MSCs using the High Pure RNA Isolation Kit
 16 (Roche Diagnostics, Mannheim, Germany), according to the
 17 manufacturer's instructions. RNA purity and concentration was
 18 quantified using NanoVue Plus spectrophotometer (GE Healthcare,
 19 Piscataway, NJ, USA). Complementary DNA (cDNA) was then
 20 synthesized from the extracted total RNA (1.6 μ g) using the
 21 Transcriptor Universal cDNA Master kit (Roche). Specific cDNA was
 22 amplified by PCR using a reaction mix (20 μ L) composed of 2 mM
 23 Tris-HCl (pH 8.0), 10 mM KCl, 0.01 mM EDTA, 0.1 mM DTT, 1 U DNA
 24 polymerase (TaKaRaEx *Taq*; Takara Bio), 0.2 mM dNTP mixture, 0.5
 25 μ M of each primer, and approximately 100 ng of cDNA template.
 26 The synthesis conditions were as follows: 94°C (45 s), 62°C (30 s),
 27 and 72°C (90 s). qRT-PCR was conducted using FastStart Essential
 28 DNA Green Master kit (Roche) and LightCycler® Nano instrument
 29 (Roche) in 15 μ L of reaction mix with cDNA, and 5 μ M each primer
 30 (*JAG1*: Forward 5' - CGGGAACATACTGCCATGAAAATA - 3', Reverse 5'
 31 - ATGCACCTGTAGGAGTTGACACCA - 3'; *GAPDH*: Forward 5' -
 32 CGTCTTACCACCATGGAGA - 3', Reverse 5' -
 33 CGGCCATCAGCCACAGTTT - 3'). The amplification conditions were
 34 as follows: 95°C (60 s) followed by 45 cycles of 95°C (20 s), 60°C
 35 (20 s), and 72°C (20 s). The levels of PCR product were standardized
 36 to that of *GAPDH* mRNA, which was defined as 1 arbitrary unit.

37 Flow cytometry

38 To analyze cell-surface expression of CD34 and CD38 marker
 39 proteins, HSPCs were labelled with anti-human CD34-FITC (clone
 40 581, BD Pharmingen, CA, USA) and anti-human CD38-PE (clone HB7,
 41 Becton Dickinson and Co. CA, USA). In brief, collected cells were
 42 resuspended in 1% BSA/PBS, and incubated with fluorescence dye-
 43 conjugated antibodies (1:25 dilution) for 1 h at 4°C. Then, cells were
 44 double stained with propidium iodide in order to exclude dead cells
 45 from the analysis and washed twice with 1% BSA/DPBS. For
 46 quantification of cell number 25 μ L (2.75 \times 10⁴ particles) of
 47 CountBright™ absolute counting beads (Invitrogen, CA, USA) were
 48 added to each sample immediately before counting. To reduce the
 49 noise of non-blood cells, the region of blood cells was determined
 50 by a FSC-SSC gating. The CD34⁺ and CD38⁺ quadrants were
 51 determined by reference to isotypic controls after compensation.
 52 Data acquisition and analysis was performed using FACSCalibur
 53 instrument (BD Biosciences, NJ, USA).

54 Colony-forming units assay

55 Hematopoietic potency of the CD34⁺ cells was examined by the
 56 colony-forming units (CFU) assay by resuspending the cells in a
 57 semi-solid methylcellulose medium (MethoCult GF H4434; StemCell
 58 Technologies, Vancouver, BC, Canada), which consisted from
 59 Iscove's modified Dulbecco's medium supplemented with 1%
 60 methylcellulose, 30% fetal bovine serum, 1% bovine serum albumin,
 61 100 μ M 2-mercaptonethanol, 2 mM L-glutamine, 50 ng mL⁻¹ stem
 62 cell factor, 10 ng mL⁻¹ GM-CSF, 10 ng mL⁻¹ IL-3 and 3 U mL⁻¹
 63 erythropoietin and seeding at a density of 10³ cells per dish.
 64 Duplicates were performed in each culture. The cells were
 65 incubated in a humidified atmosphere with 5% CO₂ at 37°C. At day
 66 14 the number of CFU was counted based on the morphology of
 67 colonies as follows: burst-forming unit-erythroids (BFU-E),
 68 granulocytes/macrophages (CFU-GM), or
 69 granulocytes/erythroid/macrophages/megakaryocytes (CFU-
 70 GEMM). At day 28, the dense colonies larger than 1 mm in diameter
 71 were counted as high-proliferative potential colony-forming cells
 72 (HPP-CFC).

73 Statistical analysis

74 All experiments were conducted at least three times, and all values
 75 were reported as the mean \pm standard deviation (SD). Statistical
 76 analysis was carried out by Welch test using R commander (Version
 77 2.1-7).

78 Results

79 The 3D skeleton of an artificial niche and its function

80 In this study, for the *in vitro* expansion of HSPCs artificial
 81 hematopoietic niches were constructed. The skeleton of the
 82 constructs was composed of overlaid electrospun fiber scaffolds
 83 with different fiber orientations that were obtained via controlling
 84 the electrospinning collector rotation speed. The constructs
 85 composed of three overlaid transversely isotropic fibers were
 86 named Scaffold-I and constructs composed of three overlaid
 87 anisotropic fibers were named Scaffold-II (Table 1). For the
 88 fabrication of Scaffold-I and II with different geometrical features,
 89 PU that is highly elastic and biocompatible was used.

90 The diameter and orientation of fabricated fibers were analyzed
 91 from SEM images. Herein nanofibers composing both scaffold types
 92 did not show significant difference in their diameters, Scaffold-I =
 93 1.72 \pm 0.52 μ m and Scaffold-II = 1.85 \pm 0.5 μ m. Fiber orientations
 94 were calculated by second-order parameter, *S*, where *S* value closer
 95 to 1 referred to a perfectly aligned fibers and *S* closer to 0 referred
 96 to a randomly oriented fibers. Second-order parameter
 97 measurement of Scaffold-I showed that nanofibers were aligned
 98 parallel (*S* = 0.96 \pm 0.02) conducting transversely isotropic properties
 99 (Fig. 1B). By contrast, in Scaffold-II, low rotational speed of the
 100 collector resulted in randomly oriented nanofibers (*S* = 0.51 \pm 0.09)
 101 resulting in anisotropic properties (Fig. 1C). SEM observations also
 102 showed that in the obtained scaffolds pores were interconnected
 103 and the average pore size of Scaffold-I and II were 32.8 \pm 43.6 μ m²
 104 and 8.6 \pm 5.5 μ m², respectively (Table 1). The average distance

1 between each layer in both scaffolds was approximately 200 μm .
 2 These results show that we have obtained geometrically different
 3 scaffolds with uniformly interconnected pores.

4 Gene expression in MSCs on biohybrid niches

5 To study the effect of scaffolds on the expression of *JAG1* in MSCs,
 6 which plays an important role in maintaining self-renewal property
 7 of HSPCs,²¹ qRT-PCR analysis was conducted. The expression level of
 8 *GAPDH* in all samples was not significantly difference. The results
 9 showed that MSCs cultured on Scaffold-II have significantly higher
 10 expression of *JAG1* gene, compared to Scaffold-I (Fig. 2), suggesting
 11 that fibrous scaffolds with anisotropic properties are capable to
 12 induce haematopoiesis supportive function in MSCs that can
 13 facilitate successful *in vitro* expansion and retention of HSPCs
 14 potential to differentiate into various lineages.

15 Expansion of hematopoietic stem/progenitor cells by using 16 layered fiber scaffolds

17 The *in vitro* expansion efficiency of HSPCs in our 3D biohybrid
 18 hematopoietic niche was studied in comparison to the cells cultured
 19 in a conventional 2D system. The proliferation activity and
 20 immunophenotype of expanded HSPCs were analyzed by CD34 and
 21 CD38 double staining and FACS analysis after 7 days of culture;
 22 where CD34 is a classical HSPCs marker,²⁵ and CD34⁺CD38⁻ cells are
 23 primitive population of HSPCs.¹³ The quantitative analysis of
 24 expanded HSPCs showed no significant difference among three
 25 groups. However, absolute cell number in both artificial niches was
 26 higher than in 2D control culture. Specifically, in 3D-I culture, $3.3 \times$
 27 10^5 cells per cm^2 were counted, in 3D-II culture 3.5×10^5 cells per
 28 cm^2 , and in 2D culture 1.8×10^5 cells per cm^2 (Fig. 3A). No
 29 significant difference was observed among these culture conditions
 30 in cell numbers.

31 Next, the cell population composition of each culture revealed
 32 that HSPCs cultured in 3D artificial niches retained their high CD34
 33 expression compared to 2D culture. CD34⁺ cell population in 3D-I
 34 culture was 2.7×10^4 cells per cm^2 , in 3D-II culture 2.5×10^4 cells
 35 per cm^2 , and only 1.1×10^4 cells per cm^2 were quantified in 2D
 36 culture (Fig. 3B). The retention of primitive CD34⁺CD38⁻ phenotype
 37 analysis also showed that cells cultured in 3D artificial niches
 38 maintained the large number of CD34⁺CD38⁻ cells (Fig. 4), 3D-I = 1.5
 39 $\times 10^4$ cells per cm^2 and 3D-II = 1.4×10^4 cells per cm^2 , after 7 days of
 40 culture. 3D cultures showed the tendency of higher number of
 41 CD34⁺CD38⁻ cells than 2D culture, however no significant difference
 42 was observed between the two 3D cultures (Fig. 3C).

43 Hematopoietic functions of CD34⁺ progeny cells

44 Hematopoietic potency of the CD34⁺ progeny cells cultured in
 45 geometrically different 3D biohybrid niches was examined by CFU
 46 assay and compared with 2D culture. Expanded cells were
 47 examined for availability of CFU-GM, BFU-E, HPP-CFC and CFU-
 48 GEMM, where HPP-CFC and CFU-GEMM are multipotential
 49 progenitors and believed to be more primitive than the lineage-
 50 restricted CFU-GM and BFU-E. Morphology of obtained colonies is
 51 shown in insets of Fig. 5. CFU assay results showed that HSPCs
 52 expanded in 2D culture, 3D-I and 3D-II cultures with 10^3 input cells

53 gave rise to 2.7, 6.2, and 9.7 CFU-GEMM colonies; 3.9, 8.5, and 10
 54 CFU-GM colonies; 3.7, 8.6, and 11.0 BFU-E colonies; respectively
 55 after 14 days of culture. After 28 days of culture 5.0, 12.7, and 16.7
 56 HPP-CFC colonies were counted (Fig. S1). The number of CFU-
 57 GEMM and HPP-CFC colonies in 3D-I culture was significantly higher
 58 than in the 2D culture indicating that our artificial hematopoietic
 59 niche is potential for maintaining multipotential properties of
 60 HSPCs. The comparison of fold change of initial cell number in 2D
 61 and 3D cultures shown in Fig. 5 revealed significant difference
 62 between these two culture systems except in formation of CFU-GM.
 63 As expected, 3D-II culture showed significantly high fold-increase in
 64 more primitive CFU-GEMM and HPP-CFC. These results show that
 65 3D cultures are able to support proliferation of HSPCs, maintain
 66 their primitive phenotype, and accommodate large number of cells
 67 in comparison to the 2D culture, suggesting that the designed
 68 artificial niches have potential to be used as an *in vitro* expansion
 69 system for HSPCs that can fulfill the clinical necessity and quality of
 70 transplant HSPCs.

71 Discussion

72 Due to the necessity for an improvement in the clinical outcome of
 73 HSPCs transplantation, the *in vitro* expansion of these cells is
 74 needed. In the 3D cultivation method of HSPCs, geometry and
 75 porosity of the scaffold are important regulatory, for the cell
 76 infiltration as well as for a distribution of soluble factors.²⁶ In this
 77 context, it was desired to mimic the bone endosteal
 78 microenvironment of BM, where HSPCs are nurtured.^{15, 27} To
 79 achieve this goal, we proposed a fabrication of 3D biohybrid
 80 hematopoietic niche composed of electrospun fiber scaffolds and
 81 MSCs as a feeder cells. Efficiency of the designed 3D biohybrid
 82 niche was compared with a conventional 2D culture system. In
 83 addition, in order to study the effect geometrical properties of the
 84 niche on proliferation capacity and functionality of expanded
 85 HSPCs, the niche composing fiber scaffolds were prepared with
 86 distinctive transversely isotropic or anisotropic properties.
 87 The first advantage of our electrospun fiber scaffolds is their
 88 microscale architecture with high surface-to-volume ratio and
 89 capacity to selectively enhance adsorption of ECM proteins that are
 90 able to modulate interactions of the cells with the environment and
 91 cell communication.²⁸ In the experimental results, HSPCs cultured in
 92 3D biohybrid niche had higher proliferative potential and
 93 multipotency than that of 2D culture system. It appears that
 94 interconnected pores and micro-topography of each layer that
 95 consisted 3D biohybrid niche resembled the natural ECM facilitating
 96 formation and maturation of cell focal adhesion and actin
 97 polymerization, which are important in MSCs osteogenesis.²⁹ Our
 98 previous study revealed that the same scaffolds with transversely
 99 isotropic and anisotropic properties can serve as a physical cue for
 100 controlling MSCs fate. MSCs seeded onto anisotropic fiber scaffolds
 101 committed to an osteogenic differentiation and were potential to
 102 deposit large amounts of calcium²² that are essential for
 103 hematopoietic niche composing feeder cells.²¹ Further coculture
 104 and methylcellulose-based CFU assay revealed superior potential of
 105 3D biohybrid niches to give rise of higher number of colonies
 106 compared to 2D culture system. In case of 3D cultures, cells of 3D-II
 107 retained their highest potential to differentiate into multilineage

1 progenitor cells and gave rise of higher number of colonies. 56 In this study, we fabricated 3D biohybrid hematopoietic niches
 2 Probably, microstructure of Scaffold-II of 3D-II more closely 57 for the expansion of clinically important HSPCs. Compared to
 3 resembled the natural ECM as well as significantly high expression 58 the conventional 2D culture system our designed 3D biohybrid
 4 of *JAG1* in the feeder cells, which an important feature of HSPCs 59 niches can facilitate niche-like microenvironment to support
 5 supporting cells,¹³ might caused the obtained results. Since, the 60 proliferation activity and retention of primitive phenotype in
 6 interaction between Notch-1 in HSPCs and Notch-1 ligand *JAG1* in 61 HSPCs. 3D biohybrid niche consisting scaffolds were able to
 7 stromal cells plays an important role in the self-renewal of HSPCs 62 control chemical signals secretion from feeder MSCs through
 8 and retention of more primitive immunophenotype.^{21, 30} These 63 mechanotransduction to facilitate successful *in vitro* expansion
 9 results are also associated with location of HSPCs according to Jing 64 and retention of HSPCs with superior potential to differentiate
 10 D et al., in conventional 2D coculture system HSPCs, which had a 65 into various lineages.

11 direct contact with MSCs, had the highest proliferation capacity; 66 Future work will be focused on the development of more
 12 however cells which migrated beneath MSCs monolayer had more 67 effective 3D biohybrid niches with higher number of fibrous
 13 primitive cells.¹⁴ However, in our results, we have observed 68 layers and applicable for microscopy observations.

14 remarkable difference between two 3D cultures (Fig. 2), but the 69
 15 difference in cell increase was insignificant. This can be attributed 69
 16 to the effect of soluble factors. It is possible that interconnected 69
 17 pores of each fiber layer of the scaffold and the space (~200 μm) in- 70
 18 between fiber layers facilitated the formation of niche-like 70
 19 microenvironment allowing specific distribution of soluble factors 70
 20 as well as MSCs and HSPCs. That is, HSPCs that came into direct 71
 21 contact with MSCs might be stimulated into high proliferation state, 71
 22 and due to their small cell size, they migrated into the second and 72
 23 third layers of MSCs, which might consequently trigger further 72
 24 proliferation. Meanwhile, the non-adherent HSPCs that existed in- 73
 25 between the fiber layers might maintain their primitive phenotype 73
 26 (Fig. 6). Therefore, increasing the number of overlaid scaffolds 74
 27 might improve the efficiency of these culture systems. 75

28 These results suggest that the structural advancement of our 76
 29 3D biohybrid niche is capable of facilitating high-density expansion 76
 30 of multipotent HSPCs. 77

31 The second important aspect of our 3D niche is its mechanical 78
 32 property. Compared to 2D culture system, cells cultured in 3D-I 78
 33 cultures had 2-fold higher number of primitive cells such as CFU- 79
 34 GEMM and HPP-CFCs (Fig. S1). The 3D-II culture showed no 79
 35 significant difference due to the effect of cord blood lots, but had 80
 36 similar tendency to 3D-I. Like BM niche, our 3D biohybrid niches 80
 37 regulate the mechanotransduction of HSPCs, where the 81
 38 involvement of actin-myosin cytoskeleton and membrane receptors 81
 39 such as integrins help them to sense their microenvironment.³¹ 82
 40 Recent study showed that substrate elasticity promotes two- to 82
 41 three fold expansion of HSPCs, probably resembling certain 83
 42 diseased state of the tissue.³² Thus we consider that elasticity of 83
 43 our scaffolds also promoted the expansion of HSPCs. 84
 44 The third important aspect of our 3D niche is its beehive-like 84
 45 structure that is easy to assemble and disassemble allowing 85
 46 efficient collection of cultured cells from each scaffold layer. In the 85
 47 assembled scaffold the distance between fiber scaffold layers 86
 48 allows sufficient exchange of nutrition and oxygen as well as the 86
 49 removal of metabolic waste of the cells. Since, in this study 3D cell 87
 50 culture experiments were carried out in a small volume static 87
 51 medium, only three layers of fiber scaffolds were used in order to 88
 52 prevent oxygen depletion. Size and structural modifications of our 88
 53 artificial niche can be done upon necessity to obtain higher than 1.7- 89
 54 × 10⁵ CD34⁺ cells kg⁻¹ to facilitate high survival of the patient.³³ 89

55 **Conclusions** 90

55 Conclusions

69 Conflict of interest

70 The authors declare no competing financial interest.

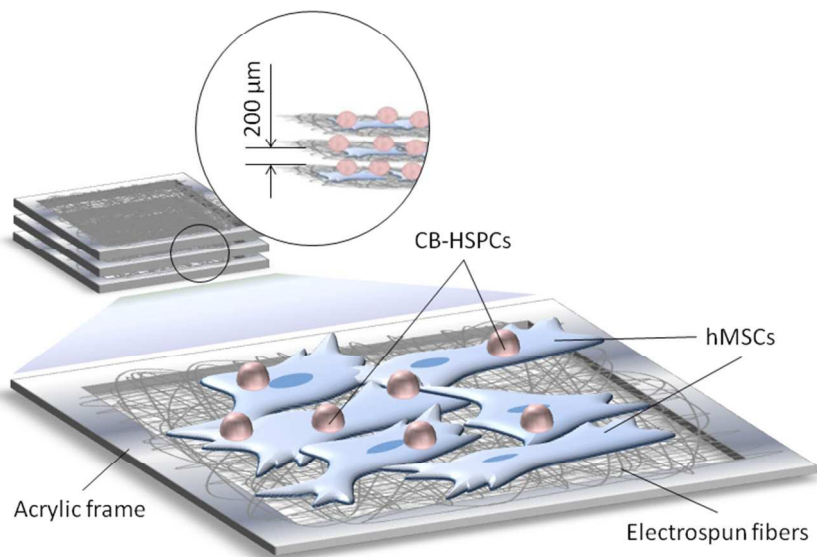
71 Acknowledgements

72 This research was partially supported by JSPS KAKENHI Grant
 73 Number 25870272 and JST A-STEP No. AS251Z02503P.

74 References

- 76 1. S. Méndez-Ferrer, T. V. Michurina, F. Ferraro, A. R. Mazloom,
 77 B. D. MacArthur, S. A. Lira, D. T. Scadden, A. Ma'ayan, G. N.
 78 Enikolopov and P. S. Frenette, *Nature*, 2010, **466**, 829-834.
- 79 2. M. Remberger, J. Mattsson, R. Olsson and O. Ringdén, *Clin.*
 80 *Transplant.*, 2011, **25**, E68-E76.
- 81 3. E. A. Copelan, *New Engl. J. Med.*, 2006, **354**, 1813-1826.
- 82 4. A. Mendelson and P. S. Frenette, *Nat. Med.*, 2014, **20**, 833-
 83 846.
- 84 5. Y. Xie, T. Yin, W. Wiegand, X. C. He, D. Miller, D. Stark, K.
 85 Perko, R. Alexander, J. Schwartz and J. C. Grindley, *Nature*,
 86 2008, **457**, 97-101.
- 87 6. N. J. Chao, S. G. Emerson and K. I. Weinberg, *ASH Education*
 88 *Program Book*, 2004, **2004**, 354-371.
- 89 7. M. J. Laughlin, M. Eapen, P. Rubinstein, J. E. Wagner, M.-J.
 90 Zhang, R. E. Champlin, C. Stevens, J. N. Barker, R. P. Gale and
 91 H. M. Lazarus, *New Engl. J. Med.*, 2004, **351**, 2265-2275.
- 92 8. S. Agrawal, Tripathi, Piyush, Naik, Sita, *Journal*, 2009.
- 93 9. M. Körbling and T. Fliedner, *Bone Marrow Transplant.*, 1996,
 94 **17**, 675-678.
- 95 10. P. Dhot, V. Nair, D. Swarup, D. Sirohi and P. Ganguli, *Indian J.*
 96 *Pediatr.*, 2003, **70**, 989-992.
- 97 11. K. Ohishi, B. Varnum-Finney and I. D. Bernstein, *J. Clin.*
 98 *Invest.*, 2002, **110**, 1165-1174.
- 99 12. V. M. Sandler, R. Lis, Y. Liu, A. Kedem, D. James, O. Elemento,
 100 J. M. Butler, J. M. Scandura and S. Rafii, *Nature*, 2014, **511**,
 101 312-318.
- 102 13. T. Walenda, S. Bork, P. Horn, F. Wein, R. Saffrich, A.
 103 Diehlmann, V. Eckstein, A. D. Ho and W. Wagner, *J. Cell. Mol.*
 104 *Med.*, 2010, **14**, 337-350.

- 1 14. D. Jing, A. V. Fonseca, N. Alakel, F. A. Fierro, K. Muller, M.
2 Bornhauser, G. Ehninger, D. Corbeil and R. Ordemann,
3 *Haematologica*, 2010, **95**, 542-550.
- 4 15. B. Guezguez, C. J. Campbell, A. L. Boyd, F. Karanu, F. L.
5 Casado, C. Di Cresce, T. J. Collins, Z. Shapovalova, A.
6 Xenocostas and M. Bhatia, *Cell Stem Cell*, 2013, **13**, 175-189.
- 7 16. L. Wang, R. Benedito, M. G. Bixel, D. Zeuschner, M. Stehling,
8 L. Sävendahl, J. J. Haigh, H. Snippert, H. Clevers and G. Breier,
9 *EMBO J.*, 2013, **32**, 219-230.
- 10 17. K. N. Chua, C. Chai, P. C. Lee, S. Ramakrishna, K. W. Leong
11 and H. Q. Mao, *Exp. Hematol.*, 2007, **35**, 771-781.
- 12 18. M. Kucia, J. Ratajczak and M. Z. Ratajczak, *Exp. Hematol.*,
13 2005, **33**, 613-623.
- 14 19. R. D. Nandoe Tewarie, A. Hurtado, A. Levi and J. A.
15 Grotenhuis, *Cell Transplant.*, 2006, **15**, 563-577.
- 16 20. T. Okamoto, T. Aoyama, T. Nakayama, T. Nakamata, T.
17 Hosaka, K. Nishijo, T. Nakamura, T. Kiyono and J. Toguchida,
18 *Biochem. Biophys. Res. Commun.*, 2002, **295**, 354-361.
- 19 21. S. Fujita, J. Toguchida, Y. Morita and H. Iwata, *Cell*
20 *Transplant.*, 2008, **17**, 1169-1179.
- 21 22. S. Fujita, H. Shimizu and S. Suye, *J. Nanotechnology*, 2012,
22 **2012**.
- 23 23. R. S. Stein and F. H. Norris, *Journal of polymer science*, 1956,
24 **21**, 381-396.
- 25 24. S. Nomura, H. Kawai, I. Kimura and M. Kagiyama, *J. Polym.*
26 *Sci 2 Polymer Phys.*, 1970, **8**, 383-400.
- 27 25. S. Kanji, M. Das, R. Aggarwal, J. Lu, M. Joseph, S. Basu, V. J.
28 Pompili and H. Das, *Stem Cell Res.*, 2014, **12**, 275-288.
- 29 26. A. Raic, L. Rödling, H. Kalbacher and C. Lee-Thedieck,
30 *Biomaterials*, 2014, **35**, 929-940.
- 31 27. M. Hines, L. Nielsen and J. Cooper-White, *J. Chem. Technol.*
32 *Biotechnol.*, 2008, **83**, 421-443.
- 33 28. X. Liu and P. X. Ma, *Ann. Biomed. Eng.*, 2004, **32**, 477-486.
- 34 29. C. H. Seo, H. Jeong, Y. Feng, K. Montagne, T. Ushida, Y. Suzuki
35 and K. S. Furukawa, *Biomaterials*, 2014, **35**, 2245-2252.
- 36 30. L. Calvi, G. Adams, K. Weibrecht, J. Weber, D. Olson, M.
37 Knight, R. Martin, E. Schipani, P. Divieti and F. Bringhurst,
38 *Nature*, 2003, **425**, 841-846.
- 39 31. C. Huang and R. Ogawa, *FASEB J.*, 2010, **24**, 3625-3632.
- 40 32. J. Holst, S. Watson, M. S. Lord, S. S. Eamegdool, D. V. Bax, L.
41 B. Nivison-Smith, A. Kondyurin, L. Ma, A. F. Oberhauser and
42 A. S. Weiss, *Nat. Biotechnol.*, 2010, **28**, 1123-1128.
- 43 33. J. E. Wagner, J. N. Barker, T. E. DeFor, K. S. Baker, B. R. Blazar,
44 C. Eide, A. Goldman, J. Kersey, W. Krivit and M. L. MacMillan,
45 *Blood*, 2002, **100**, 1611-1618.



Biohybrid hematopoietic niche for expansion of hematopoietic stem/progenitor cells
254x190mm (96 x 96 DPI)

Table 1 Parameters of obtained scaffolds

	Scaffold geometry	Second-order parameter, S	Fiber diameter (μm)	Pore size (μm^2)
Scaffold-I	Transversely isotropic	0.96 ± 0.02	1.72 ± 0.52	32.8 ± 43.6
Scaffold-II	Anisotropic	0.51 ± 0.09	1.85 ± 0.5	8.6 ± 5.5

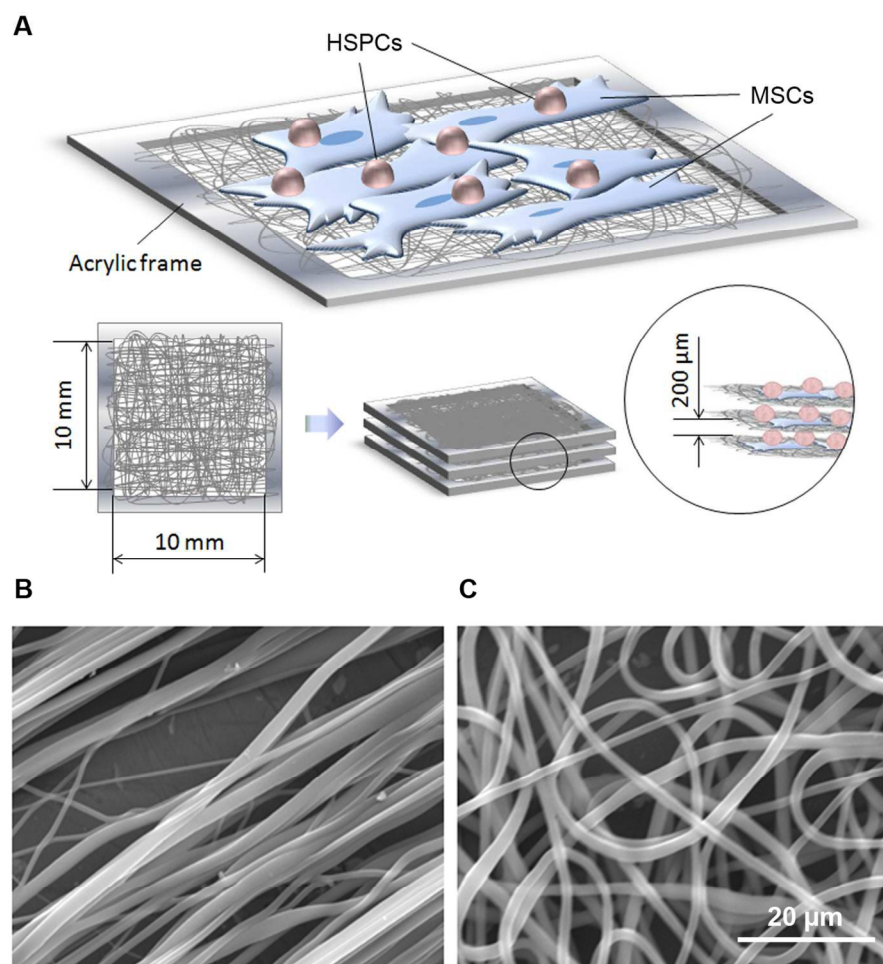


Figure 1 A. Schematic image of biohybrid hematopoietic niche. B. SEM image of transversely isotropic Scaffold-I. C. SEM image of anisotropic Scaffold-II. 111x144mm (300 x 300 DPI)

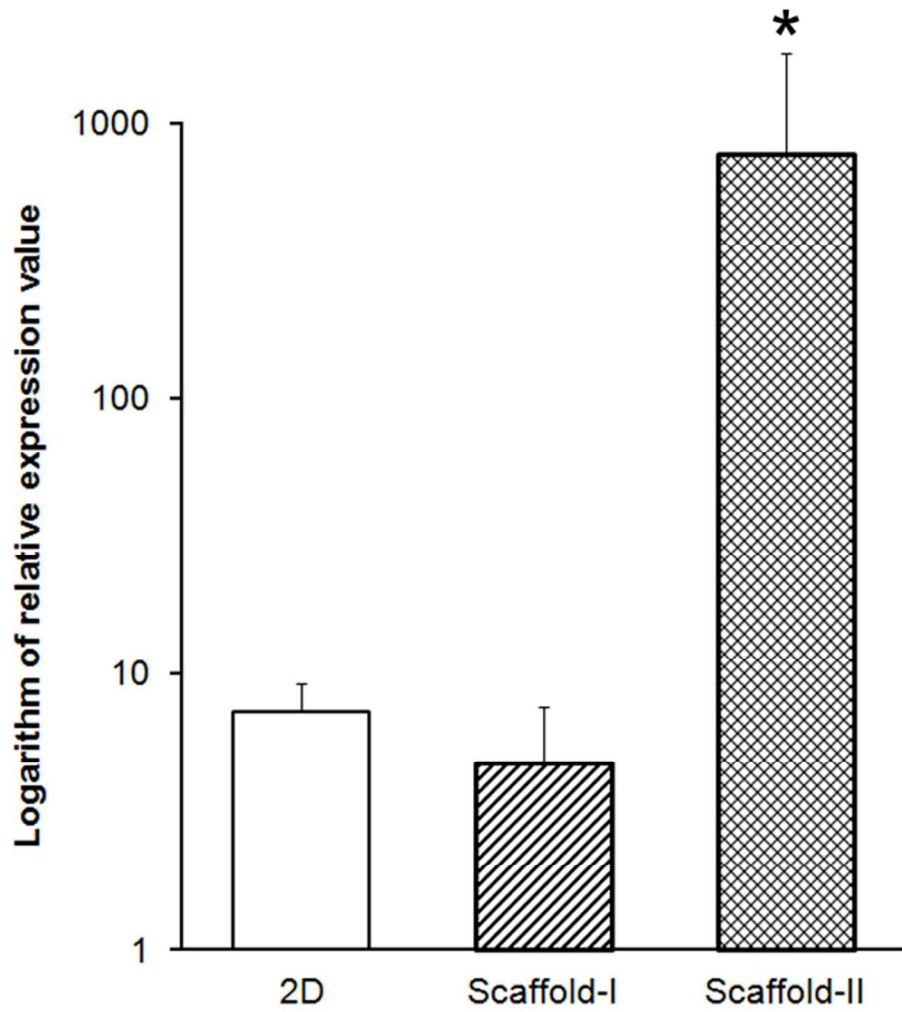


Figure 2 JAG1 expression in MSCs cultured on artificial niches. An asterisks represents significant difference (* $p < 0.05$)
59x67mm (300 x 300 DPI)

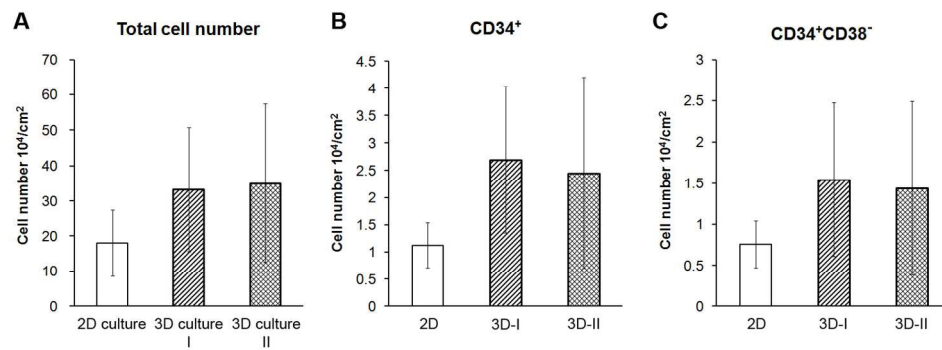


Figure 3 A. Quantification of total cell number in different culture conditions after 7-day coculture. B. Total number of CD34⁺ cells, C. Total number of CD34⁺CD38⁻ cells. Mean \pm SD (n=3). 140x51mm (300 x 300 DPI)

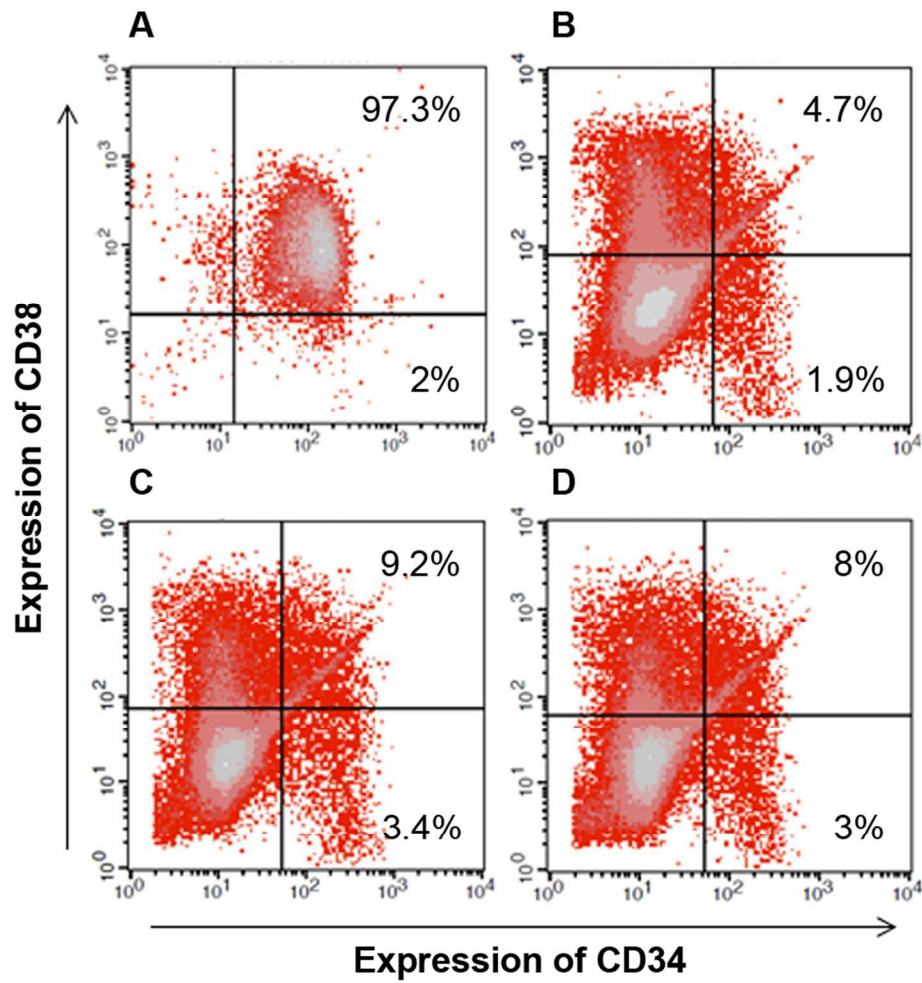


Figure 4 CD34/CD38 expression in relation to the number of HSPCs after 7-day coculture. A. CD34⁺ cell fraction before coculture, B. Expanded cells cultured in 2D culture system, C. in 3D culture-I and D. in 3D culture-II.

90x94mm (300 x 300 DPI)

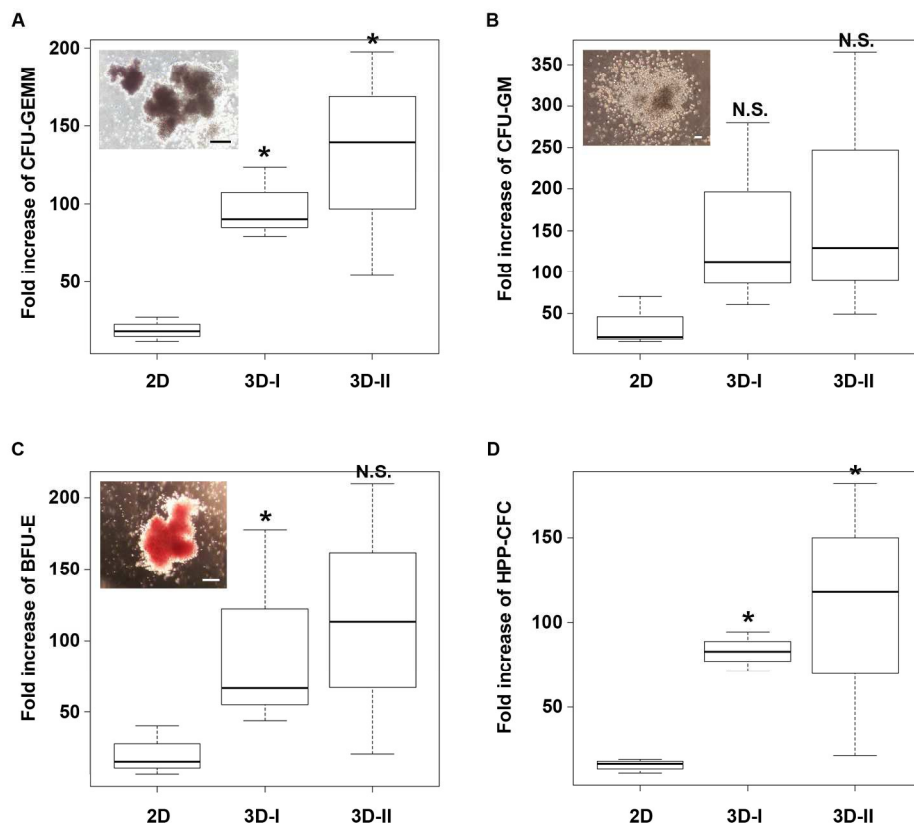


Figure 5 Hematopoietic potency of the CD34+ cell progeny after 14 days of culture in different culture systems represented in cell fold increase against cell number before culture. A. CFU-GEMM (granulocytes/erythroid cells /macrophages/megakaryocytes), B. CFU-GM (colony-forming unit-granulocyte/macrophages), C. BFU-E (burst-forming unit-erythroids), D. HPP-CFC (high-proliferative potential colony-forming cells) after 28 days culture. The box plot represents the maximum, the median and the minimum of values (n=3). An asterisks represents significant difference from the control 2D culture (*p < 0.1). Insets are representative colony images (Scale bars 100 μm).
187x168mm (300 x 300 DPI)

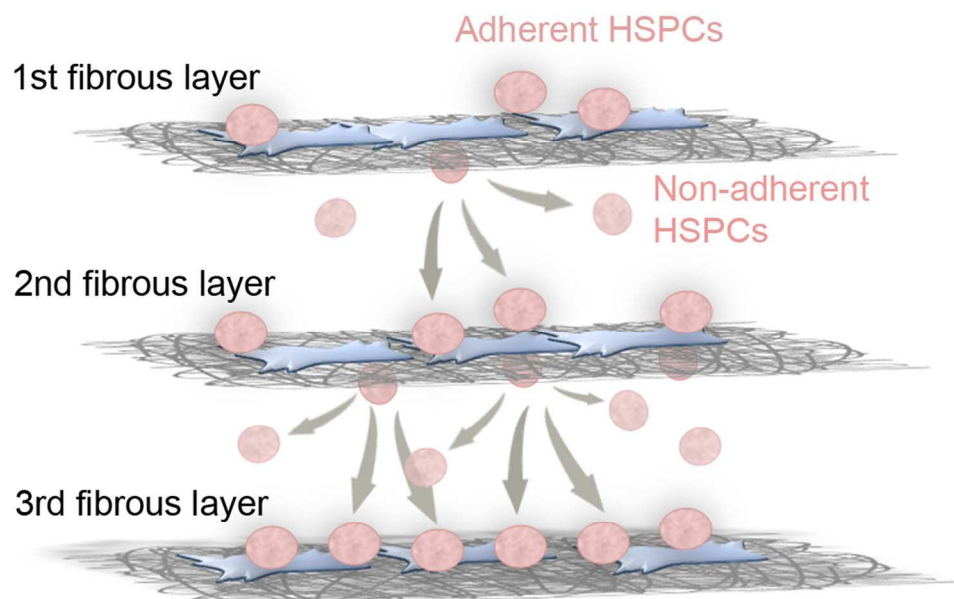


Figure 6 Proposed mechanism of the retention of HSPCs proliferative and primitive phenotype in 3D beehive-like biohybrid niche.
99x76mm (300 x 300 DPI)